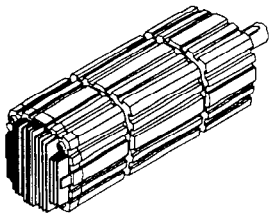

Nancy, France
4 - 6 June 1996

ANALYSIS OF TORQUE AND CURRENT RIPPLE OF AN INVERTOR DRIVEN SQUIRREL CAGE INDUCTION MOTOR BY SIMULATIONS USING AN EXTENDED MOTOR MODEL

R. De Weerdt*, E. Tuinman*, K. Hameyer**, R. Belmans**

* Holec Machines & Apparaten, Ridderkerk, the Netherlands
** Katholieke Universiteit Leuven, Dept. EE, ESAT/ELEN, Kard. Mercierlaan 94, 3001 Leuven, Belgium

Abstract - The paper describes the simulation of invertor-motor interaction emphasising the generated torque and current ripple due to non-sinusoidal supply voltage (invertor) and harmonics due to slotting and saturation (motor). In the classical analysis of induction motor, the influence of slotting and saturation is analysed by describing the airgap field as a combination of different harmonic components. In this paper, slotting and saturation are described by introducing harmonic components of the self and mutual inductances of the different phases of the motor. It is shown that the assumptions made to obtain the standard two phase model using the Park transformation are not valid when slotting and saturation are considered. Therefore, an extended motor model (13 phases), calculated using 2D finite elements is used instead of the conventional two phase model.

Keywords: Squirrel cage induction motor, simulation, extended motor model

INTRODUCTION

To analyse the behaviour of squirrel cage induction motors, several approaches are described in literature. The simulation of squirrel cage induction motors behaviour is mainly performed using two phase models either in a stationary co-ordinate system (α-β model) or in a rotating co-ordinate system (d-q model) [1]. Parasitic effects (slotting, saturation, etc.) causing torque and current ripple, are not included in these simulations.
The analysis of slotting and saturation is performed by an analytical calculation of the airgap field. Several approximations and a known current distribution are assumed. The next logical step is to describe the parasitic effects in the motor model in order to analyse their influence on the motor behaviour. This is however not possible using the two-phase models due to the approximations made during the derivation of these models. On the other hand, the description of the airgap field as a combination of different harmonic components does not provide a model that can be used in simulations.
In general, current and torque ripple are caused by:

1) Non sinusoidal supply voltage.
2) The distributed nature of the windings.
3) Non uniform airgap (slotting, saturation, eccentricity).

Both 2) and 3) are internal sources of current and torque ripple and have to be included in the motor model. First, a short overview of the basic principles of the simulation using two phase models and the analysis of the airgap field and their limitations is given.

Induction motor simulation using two phase models

These models are obtained by performing the Park transformation on the set of differential equations describing the stator and rotor phases. This results in a set of two stator- and two rotor equations. The transformation can only be applied when all rotor and all stator phases are identical. For this to be true, the following is assumed:

1) Stator and rotor surface are smooth.
2) The permeability of the iron core is constant.
3) The current distribution is considered sinusoidal along the airgap contour.

These assumptions immediately eliminate several causes of torque and current ripple. As shown below, due to the distributed nature of the windings, the slotting and saturation, the assumption that the different phases are identical is only true in a global, averaged sense. Instantaneously, the different phases are not identical.

Analysis of the airgap field

The analysis of torque and current ripple as described in the literature is based on the determination of the

airgap field. The airgap field is described as a combination of harmonic components [2]. The analytical expression of the airgap field is derived for a known current distribution. In practice however, the voltage applied to the windings is known, while the current (and it's harmonic content) are the unknown. Furthermore, several assumptions and simplifications are used to obtain the analytic expression of the airgap field. Distinction is made between harmonics due to the distributed nature of the winding and harmonics due to non-uniformity's of the airgap.
The harmonic content of the airgap field due to the distributed nature of the winding is obtained as follows:

1) The stator and rotor are assumed to be smooth. The number of ampere-turns in each slot is replaced by a current layer, infinitely thin, located at the slot opening.
2) The stator and rotor iron are assumed to be perfectly magnetically conducting ($\mu_r = \infty$).

Using these assumptions, the airgap field can be approximated analytically using the Ampères Law:

$$\oint \vec{H} d\vec{l} = I, \qquad (1)$$

where I represents the current distribution. The following figure shows the winding layout of a motor having a two layer winding with two slots per pole and per phase. The windings are short-pitched by one slot (figure 1).

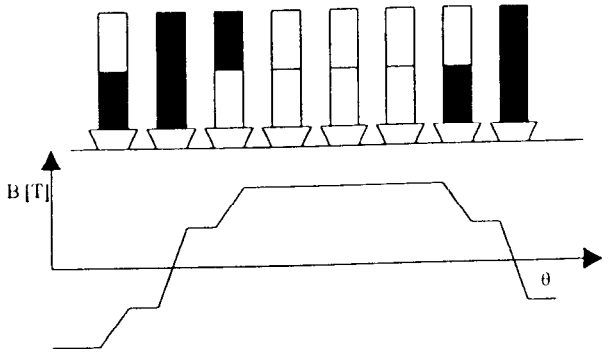

Figure 1: Winding layout, current distribution and approximated airgap field generated by a current in one of the stator phases.

The current distribution and the airgap field derived from this current are shown. Only a current in one of the stator phases is assumed. The obtained field is not sinusoidal but contains an infinite number of harmonics of order υ:

$$\upsilon = 1 + 2g \qquad g = 0, \pm 1, \pm 2, \ldots \qquad (2)$$

Only odd harmonic components are present in the spectrum of the airgap field. When a three phase, symmetric current system is assumed, all multiples of three also disappear from the spectrum. Each harmonic induces an infinite set of harmonics in the rotor. The interaction between the different harmonic field components gives rise to parasitic effects such as asynchronous torques, synchronous torques and ripple torques.
The effects of slotting, saturation or eccentricities are included in the analysis in a similar way. The airgap width δ at an angle β along the stator is described as a function of time t and rotor position θ:

$$\delta = \delta_0 + \delta_s (1 + \cos(\beta * N_s)) + \delta_r (1 + \cos((\beta + \theta) N_r)) \qquad (3)$$

Here δ_0 is the minimal airgap length, N_s and N_r are the number of stator and rotor slots. θ is the angle between the stator and rotor reference frame. δ_r and δ_s describe the variation of the airgap width and are a function of the actual slot shapes. Using this expression for the airgap width (3), the airgap field can be expressed analytically using (1). From this expression, amplitudes and frequencies of torque and current harmonics are obtained.
This analysis however has several drawbacks. Due to the assumptions made, the harmonic content of the derived airgap field is only valid in a qualitative way. They do not allow the amplitudes of the harmonics in torque or current to be predicted accurately. Furthermore, the airgap field analysis is completely separated from the simulations using the two-phase models: The airgap field analysis gives an approximation of the parasitic effects encountered in the induction motor, but the influence on the dynamic behaviour of the motor cannot be examined. The two phase models described above, allow the simulation of the dynamic behaviour, but all parasitic effects had to be neglected to obtain the model. In order to simulate the motor behaviour a motor model is required including these parasitic effects.

Extended motor model

Instead of trying to include the parasitic effects into the two phase models, the starting point to obtain the required model is the general notion that an induction motor, or any other electromagnetic device, can be thought of as a set of coupled windings described by a set of voltage differential equations:

$$[u] = [R][i] + \frac{d}{dt}[\psi] \quad , \qquad (4)$$
$$[\psi] = [L][i]$$

where [R] is the resistance matrix, [i] the current vector, [u] the applied voltage vector, [ψ] the vector describing the flux linkages and [L] the inductance matrix. The inductance matrix [L] describes the self- and mutual inductances between all phases (or

windings) considered. From this point on, the analysis is restricted to induction motors having an integer number of slots per pole and per phase for the stator and an integer number of slots per pole for the rotor. If eccentricity is not considered, it is sufficient, for the given circumstances, to treat only one pole of the motor. As a rotor phase, either a single rotor bar or the loop formed by two adjacent rotor bars and two ring segments can be considered. As the motors used in the calculations and simulations have four poles, 48 stator slots and 40 rotor slots, the extended model consists of 3 stator phases and 10 rotor phases.

INDUCTANCE MATRIX

In order to be able to simulate the motor behaviour, the inductance matrix [L] has to be calculated. Since some of the parasitic effects are related with the relative position between rotor and stator, this calculation has to be performed for different rotor positions. The inductance matrix can be calculated analytically using the expression of the airgap field or using a finite element approach.

Analytical calculation of the inductance matrix

The calculation of the inductance matrix is straightforward when the airgap field is described as above. The calculation is done in two steps:

1) Calculate the airgap field for a unit current in one of the phases.
2) Calculate the flux linked with each of the other phases by integration of the airgap flux density over the area of the different phases.

Because a unit current is assumed, this procedure results in one row or column of the inductance matrix. It has to be repeated for each of the phases and for different rotor positions.
The analytical approach still has the same drawbacks as the analytical calculation of the airgap field. Several approximations are made to obtain this field, so this approach does not provide us quantitative data. Nevertheless, some interesting conclusions can be drawn from this approach. Referring to the way the distributed nature of the winding (see figure 1) is described, the following conclusions can be drawn:

1) The self inductances of the different phases are constant, independent of the rotor position θ.
2) The mutual inductance between two stator phases of two rotor phases is also constant.
3) The mutual inductance between a rotor and a stator phase is non-sinusoidal but contains the same harmonics as the airgap field (2).

Both 1) and 2) are explained by the fact that, assuming a sinusoidal varying current in one of the phases, the flux density at each point in the airgap varies sinusoidal. As for the mutual inductance between a rotor and a stator phase, it is clear that the flux density integrated over the area of one winding will only vary sinusoidally if the current density distribution of the other winding is sinusoidal.
It can thus be concluded that the non-uniform current distribution is described by a non-sinusoidal mutual inductance between rotor and stator. As a consequence of 1) and 2) it can be stated that any ripple noticed in the self inductances or mutual inductances between two stator phases or two rotor phases must have it's cause due the non-uniform airgap, but is not due to the non-uniform current distribution.

Finite element calculation of the inductance matrix

For the calculation of the inductance matrix [L], a two dimensional finite element analysis is used. The finite element model describes one pole of the motor. The advantages of the finite element approach are that the actual geometry is taken into account as well as saturation. The calculation is performed in two steps. First, the instantaneous reluctivity in each element of the model for a given excitation and rotor position is calculated. This is performed using an iterative process of time-harmonic and static solutions [3]. This procedure is found to give similar results when compared to other methods described in the literature [4]. Using the extracted reluctivities, the inductance matrix [L] is calculated:
For each of the 13 phases, a linear problem is defined with a current of 1 A per phase. The problem is solved using the extracted reluctivities as an operating point and the fluxes linking the 13 phases are determined. Since a unit current of 1 A is used, these flux linkages immediately represent the self and mutual inductances of the motor. The inductances can be calculated as described above, by integrating the flux density over the area of the different phases. This leads to inaccuracies since the flux density is obtained as $\vec{B} = curl(\vec{A})$. Therefore, the inductances are calculated directly from the vector potential $\vec{A}$ [5]. This calculation is repeated for different rotor positions, the excitation is varied according to each new rotor position. Figure 2 shows the calculated self inductances of the three stator phases as a function of the rotor position. Clearly, the assumption of identical phases, prerequisite to the transformation to a two phase system does not hold and is only true in an averaging sense. Analysing the inductances using a discrete Fourier transformation, the

most important harmonics are shown to be the 2nd, 20th, 22th and 24th harmonics. The second harmonic is explained as a consequence of saturation, the other harmonics are due to slotting.

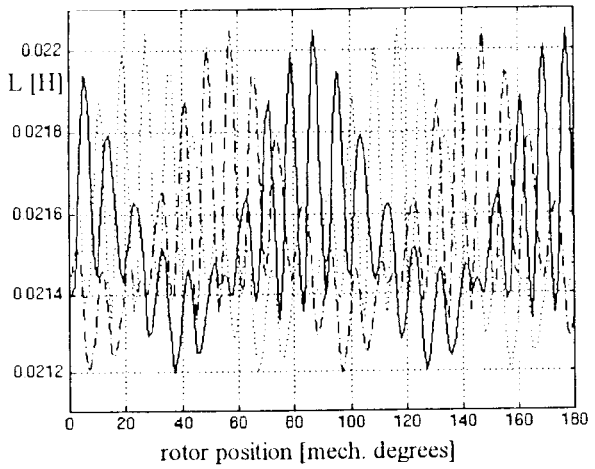

Figure 2: Variation of the self inductance of the three stator phases as a function of the rotor position.

Therefore, the self inductance of a stator phase L_s can be expressed as:

$$L_s = L_0 + L_2\cos(2\omega_n + \alpha_2) + L_{20}\cos(20p\theta + \alpha_{20}) + L_{22}\cos(22p\theta + \alpha_{22}) + L_{24}\cos(24p\theta + \alpha_{24}) \quad (5)$$

The harmonic component due to saturation is not decribed as a function of the rotor position but as a function of twice the pulsation since the flux revolves at synchronous speed. Figure 3 shows the mutual inductance between a stator and a rotor phase both in time and frequency domain.

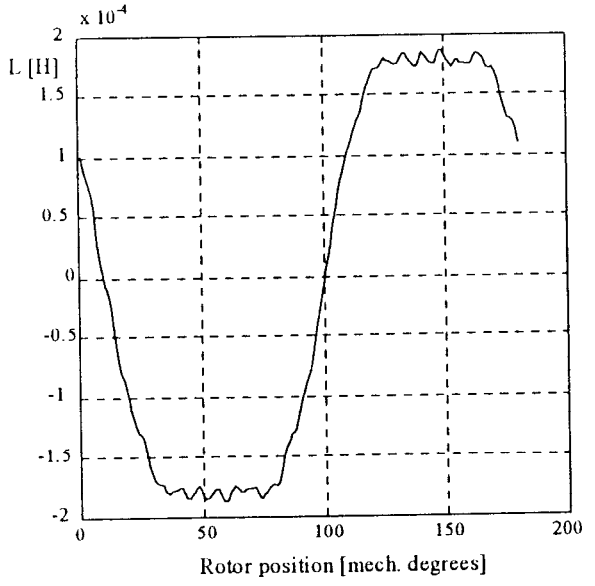

(a)

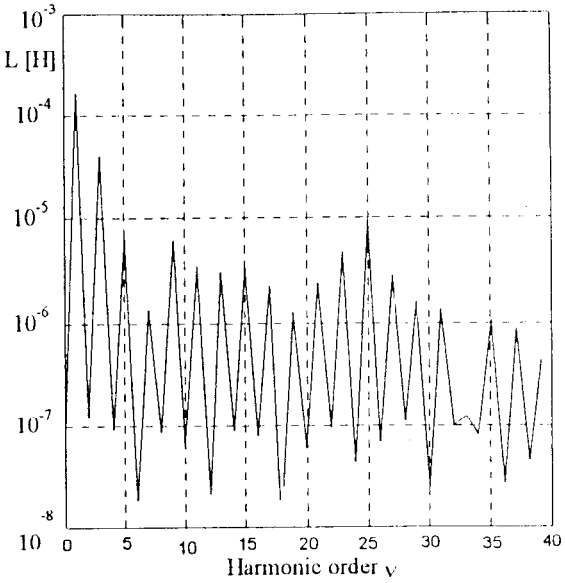

(b)

Figure 3: Variation of the mutual inductance between a rotor and a stator phase as a function of the rotor position in time-domain (a) and frequency domain (b).

A similar procedure is used to express the other elements of the inductance matrix. Using this approach, the effects of saturation and slotting are incorporated in the motor model in a natural and realistic way.

SIMULATIONS

Using the procedure described above, the inductance matrix [L] is expressed as a continuous function of time and rotor position. The set of equations (4) can be solved using standard integration techniques (Runge-Kutta, Newton-Raphson,...). Since there are two unknown in (4), flux [ψ] and current [i], the set of differential equations to be solved can be described using either of these unknown (6,7).

$$\frac{d[i]}{dt} = [L]^{-1}\left([u] - [R][i] - \frac{d[L]}{dt}[i]\right) \quad (6)$$

$$\frac{d[\psi]}{dt} = [u] - [R][L]^{-1}[\psi] \quad (7)$$

Considering the flux vector as unknown (7) has several advantages.

1) Clearly from (6) and (7), the equation is simplified when the fluxes are considered the unknowns because the derivatives of the inductance matrix are not required. In the d-q model, this is overcome by

considering the equations in a rotating reference frame. By doing so, the sinusoidal variation of the mutual inductance between stator and rotor is removed. Since none of the inductances in the matrix [L] varies sinusoidal, such transformation cannot result in a constant matrix, so d[L]/dt will not disappear in the extended model.

2) Considering the flux as unknown results in a more stable numerical integration. This is explained by the following physical consideration. The flux linking a winding is directly related with the stored magnetic energy in the winding. Therefore, rapid changes in the flux (changes that would result in a small integration step or loss of accuracy) are physically not possible. Current changes on the other hand can be very rapid. The current through a winding changes inversely proportional to the inductance change in order to maintain the flux.

3) Considering the fluxes as unknowns provides the possibility of a more accurate description of saturation. As shown above, saturation introduces a second order harmonic component. The amplitude of this harmonic can immediately be taken from the discrete Fourrier transformation and used to describe the saturation as in (5). However, a more general description, valid for different operating conditions, requires that the inductance is expressed as a function of the saturation level in each winding. In order to do this, the logical choice is to describe the inductance as a function of the flux linking the winding and not as a function of the current through it. This is illustrated by the fact that the no-load current results in a higher level of saturation than at full load, although the rated current is much higher than the no-load current.

The extended motor model is used in a similar way as the conventional two phase model. It can be used to analyse both steady-state and dynamic behaviour. By describing the inductances as a combination of harmonic components, the model has a high flexibility. The influence of each hamonic component can be considered individualy by including or neglecting it in the simulations. Two kinds of simulations are performed: at constant speed, and during speed variations, i.e. including the equation of motion. The full set of equations to be solved when motion is included becomes:

$$\begin{aligned} \frac{d[\psi]}{dt} &= [u] - [R][L]^{-1}[\psi] \\ \frac{d\theta}{dt} &= \omega \\ \frac{d\omega}{dt} &= \frac{T - T_{load} - B\omega}{J} \end{aligned} \qquad (8)$$

Here, J is the moment of inertia, $B\omega$ is the torque due to friction, T_{load} is the load torque and T is the motor torque. As mentioned in the introduction, an additional cause of torque and current ripple, is the use of a non-sinusoidal supply voltage. In order to examine the influence on the motor behaviour, several voltage wave-forms are used for the simulations. Figure 4 shows two of the wave-forms [u] used.

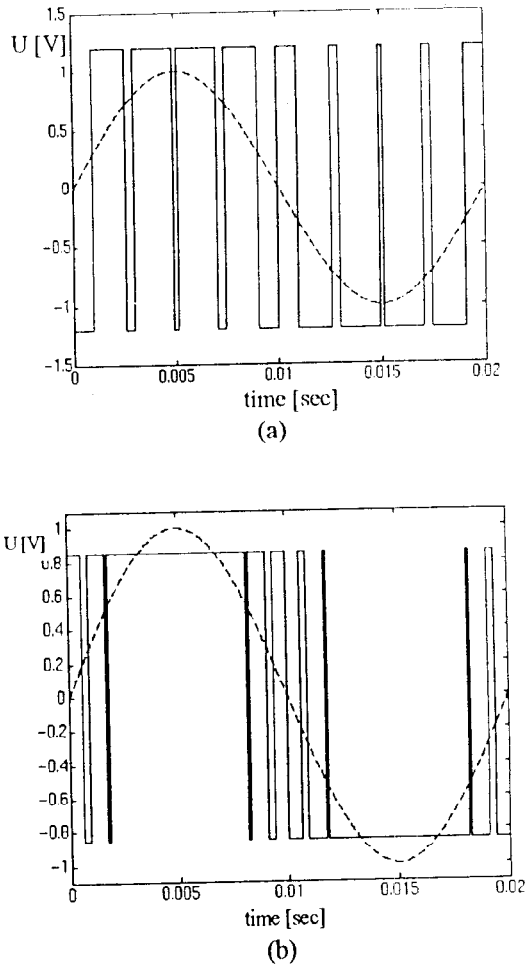

Figure 4: Wave forms in the simulations, (a) sinusoidal modulated PWM, (b) optimised PWM eliminating harmonics 5, 7, 11, and 13.

The dotted line in figure 4 represents the first harmonic of the wave form. The analysis of torque and current ripple is performed in both time and frequency domain.

RESULTS

Figure 5 shows the no-load current in the time domain using the wave shapes of figure 4. As can be seen, the optimised PWM wave form results in a more sinusoidal current than the sinusoidal modulated voltage.

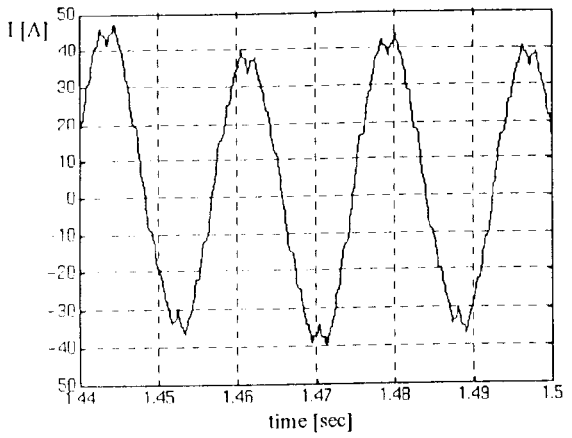

(a)

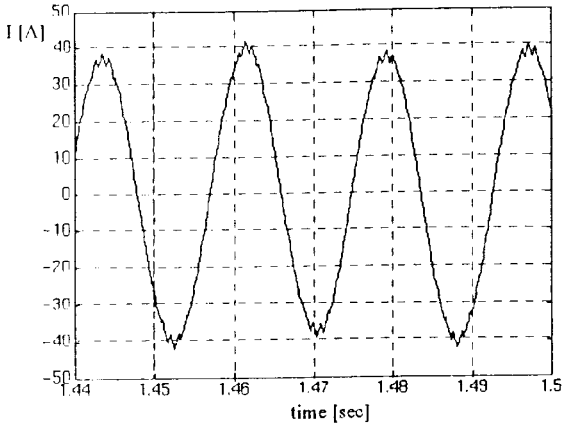

(b)

Figure 5: No-load current in time domain for sinusoidal modulated PWM (a) and optimised PWM (b).

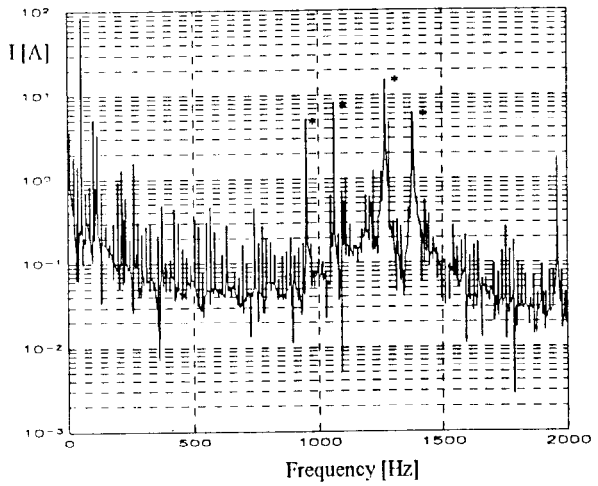

Figure 6: Frequency spectrum of rated current with optimised PWM supply.

Figure 6 shows the current spectrum at rated load for optimised PWM (figure 4.b). The harmonics in the spectrum indicated with * are due to slotting. The frequencies of the harmonics are 1050, 1162, 1271 and 1383 Hz. These frequencies are obtained by an interaction of the supply frequency (56 Hz) and a 40^{th} and 48^{th} harmonic of the mechanical frequency (27.64 Hz).

CONCLUSIONS

Squirrel cage induction motor simulations are performed using sinusoidal and non-sinusoidal voltage supply. An extended motor model is calculated using two dimensional finite element methods. Parasitic effects that are normally described by a combination of airgap field harmonics are now included in the motor model. The effects of saturation and slotting are translated into harmonics in the self and mutual inductances on the different phases. The model originates from the same set of voltage differential equations as the α–β model or d-q model. Therefore, similar integration procedures as for the two phase model are applied. The analysis is focussed on squirrel cage induction motors, but the described method is generally applicable to electromagnetic devices that can be described as a set of coupled windings. The influence of slotting, saturation and the applied wave form are analysed both in time and frequency domain.

ACKNOWLEDGMENTS

The authors are indebted to the Belgian "Nationaal Fonds voor Wetenschappelijk Onderzoek" for its financial support for this work and the Belgian Ministry of Scientific Research for granting the project IUAP No. 51 on "Magnetic Fields".

REFERENCES

[1] J. B. Woudstra, W. Deleroi and A. A. Fahim: "Simulation induction motor fed by a voltage source inverter with analytical calculation method", European Conference on Power Electronics and Applications, Aachen Germany, October 9-10 1989, pp. 227-231.

[2] Liwschitz-Garik, "Alternating Current Machines", D. Van Nostrand Company Ltd, 1946.

[3] R. Belmans, R. De Weerdt and E. Tuinman, "Combined field analysis techniques and macroscopic parameter simulation for describing the behaviour of medium-sized squirrel-cage induction motors fed with an arbitrary voltage," EPE Brighton, September 1993, pp. 413-418.

[4] E. Vassent, G. Meunier, J.C. Sabonnadière, "Simulation of induction machine operation using complex magnetodynamic finite elements," IEEE Trans. on Magnetics, Vol. 25, No. 4, 1989, pp. 3064-3066.

[5] Lowther D.A. and Silvester P.P.: "Computer-Aided Design in Magnetics," Springer-Verlag, New York, 1985.